Original Article | Journal of Biosystems Engineering

J. Biosyst. Eng. 43(4):263-272. (2018. 12)
https://doi.org/10.5307/JBE.2018.43.4.263

eISSN : 2234-1862
pISSN : 1738-1266

Analytical Study on Improvement in Load Sharing for Planetary Gear Set using Floating Ring Gear

Woo-Jin Chung[1], Kyujeong Choi[1], Jooseon Oh[1], Young-Jun Park[1,2]*, Ki-Hun Lee[3]

[1]*Department of Biosystems & Biomaterials Science and Engineering, Seoul National University, Seoul, 08826, Korea*
[2]*Research Institute of Agriculture and Life Sciences, College of Agriculture and Life Sciences, Seoul National University, Seoul, 08826, Korea*
[3]*R&D Team, SEIL Industrial Co., Ltd., Jinju, 52607, Korea*

Received: November 5th, 2018; Revised: November 13th, 2018; Accepted: November 14th, 2018

Abstract

Purpose: The load on the planet gear of a planetary gear set is uniformly distributed. However, manufacturing and assembly errors cause uneven load sharing in the planetary gear set. To solve this problem, most studies have suggested applying a floating sun gear to the planetary gear set. However, the effect of the floating ring gear and floating carrier has not been extensively studied. This study aimed to investigate the effect of the floating ring gear. **Methods:** Two models were developed; one was the fixed ring gear model, and the other was the floating ring gear model. In the fixed ring gear model, the clearance between the ring gear and the housing was 0 μm, and in the floating ring gear model, the clearance was from 10 μm to 100 μm. The load sharing of the planetary gear set was evaluated by the load sharing factor. **Results:** Our study showed that with increase in clearance, the load sharing factor of the planetary gear set approached unity. In addition, when the clearance increased above a certain level by which a fully floating ring gear was achieved, the load sharing factor was not affected by the clearance. **Conclusions:** This indicates that the fully floating ring gear increased the power density of the planetary gearbox by uniformly dividing the load of the planetary gear set. For this reason, the size of the gearbox could be decreased by using a fully floating ring gear.

Keywords: Floating ring gear, Load sharing, Planetary gear set, Power density

Introduction

Forklifts can be categorized into LPG engine forklifts, diesel engine forklifts, and electric forklifts, depending on the power source. For many years, diesel engine forklifts have generally been used in many industries because of their high durability and high torque output. In recent years, however, the demand for electric forklifts that do not emit exhaust gas has increased, as the need for the use of forklifts in indoor workplaces, such as factories, industrial facilities, agricultural facilities, has increased (Kim et al., 2011).

For most industrial vehicles, including forklifts, regardless of the type of power source, planetary gearboxes are used (Park et al, 2010; Kim and Cho, 1997; Bayindir et al., 2011). Though planetary gear sets have smaller gear sizes than those of a spur gear set or helical gear set, they transmits more power than those other gear sets. In other words, planetary gear sets have high power density. The planetary gear set has been actively studied (Shin et al., 2016; Noh et al., 2017). To achieve long life for the planetary gear set, with the advantages of miniaturization and low weight, the load sharing should be uniform (Kim et al., 2017). Therefore, the life of the planet gear could be improved by optimizing the load sharing by reducing the volume and weight of the planetary gearbox in a drive system. In addition, when the size of the drive system is reduced, the efficiency of the motor is improved. However,

***Corresponding author:** Young-Jun Park
Tel: +82-2-880-4602; **Fax:** +82-2-873-2049
E-mail: yjpark95@snu.ac.kr

due to manufacturing and assembly errors, uneven load sharing occurs in the planetary gear set, which reduces the life of the gears. Much research has been conducted on ways to improve uneven load sharing in planetary gear sets (Kim et al., 2017; Iglesias et al., 2017; Park et al., 2012; Kahraman, 1994; Nejad et al., 2015; Bodas and Kahraman, 2004; Kahraman and Vijayakar, 2001; Singh, 2010).

The simplest and most common method used to improve the load sharing in planetary gear sets is the use of floating (Iglesias et al., 2017; Park et al., 2012; Singh, 2010). Floating is a configuration in which one or more than two elements of the major components of a planetary gear set, such as the sun gear, carrier, or ring gear, are allowed to move freely in the radial direction of the nominal position without being restricted to the bearing (Park et al., 2012). Kahraman (1994) developed a non-linear time-varying (NTV) dynamic model to analyze the dynamic load sharing characteristics of a typical planetary gear set with an arbitrary number of planet gears. The results showed that the runout error of the pinion and the position error of the pinion pin have significant influence on the dynamic load sharing factor. It was also found that the floating sun gear greatly improved the dynamic load sharing characteristics. Nejad et al. (2015) analyzed the effect of eccentricity and misalignment of a planet gear on a planetary gear set, using a fixed sun gear model and a floating sun gear model. The floating sun gear improved the misalignment of the planetary gears. Kahraman and Vijayakar (2001) investigated the effect of a flexible ring gear on the quasi-static behavior of a planetary gear set. The flexible ring gear helped to improve the load sharing of the planetary gear set, but its effect was smaller than that of the floating sun gear. Singh (2010) developed a generalized formula for a planetary gear set and calculated the degree of floating necessary to make the planetary gear set a complete floating system. In addition, it was confirmed that a degree of floating above a certain level does not affect the load sharing of the planetary gear set.

Numerous studies on floating have confirmed that the load sharing of a planetary gear set could be improved with a floating sun gear. However, few studies have been conducted regarding how the load sharing of a planetary gear set could be improved when a floating carrier or a floating ring gear is used in the planetary gear set. As a result, in this study, we applied a floating ring gear to a planetary gear set that is used in the drive system of an electric forklift to investigate through simulation the effect of the floating ring gear on load sharing. To confirm this, we created two planetary gearbox simulation models. In one model, the ring gear was fixed to the housing. In the other model, the ring gear was allowed to float by the application of a radial clearance between the ring gear and the housing. To confirm the condition that the ring gear of the planetary gear set fully floats, the load sharing of the planetary gear set was calculated while the size of the clearance gradually increased.

Materials and Methods

Specification of planetary gearbox

The planetary gearbox used in this study is a drive reducer of electric forklifts. The planetary gearbox consists of two stages. There is a parallel shaft gear set in the first stage and a planetary gear set in the second stage. The power is input to the helical gear of the parallel shaft gear set and output to the carrier of the planetary gear set, while the ring gear is fixed to the housing. The rated torque and speed of the input shaft is 204 Nm @ 1000 RPM.

Figure 1 shows the electric forklift used in this study

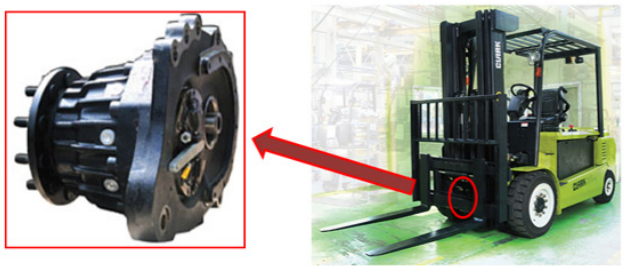

Figure 1. Illustration of the electric forklift and the drive reducer.

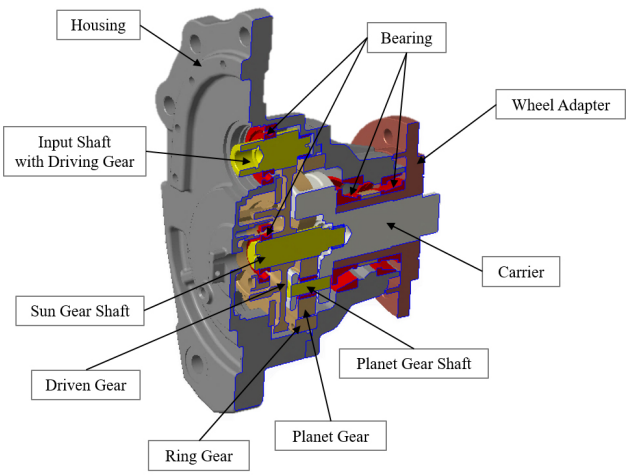

Figure 2. Section view of the planetary gearbox.

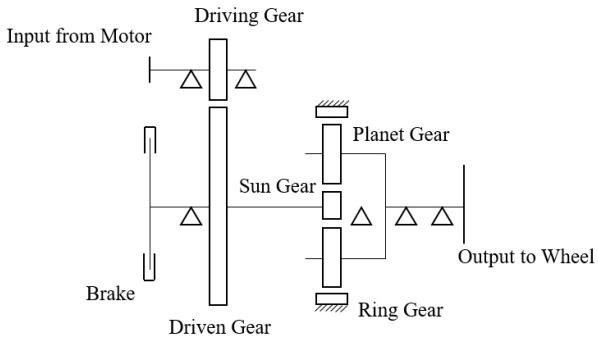

Figure 3. Schematic arrangement of the planetary gearbox.

Table 1. Specification of gears in the parallel stage

Items	Stage 1	
	Drive	Driven
Module (mm)	2.5	
Pressure angle (°)	20	
Center distance (mm)	161	
Number of teeth	26	102
Tip diameter (mm)	69.954	262
Pitch circle diameter (mm)	65.406	256.594
Root diameter (mm)	58.750	250.796
Face width (mm)	30	25
Number of gear	1	1

Table 2. Specification of gears in the planetary stage

Items	Stage 2		
	Sun	Planet	Ring
Module (mm)	3.0		
Pressure angle (°)	20		
Center distance (mm)	49		
Number of teeth	10	21	55
Tip diameter (mm)	35.134	74.000	161.569
Pitch circle diameter (mm)	31.613	63.458	158.529
Root diameter (mm)	22.500	61.366	175.069
Face width (mm)	35	25	31
Number of gear	1	3	1

and the position and shape of the driving reducer mounted on the electric forklift. It is located on the front drive axle of the forklift and driven by the motor. Figure 2 and Figure 3 provide a cross-sectional view and the gear arrangement of the planetary gearbox. Table 1 and Table 2 present the specifications of the parallel shaft gear set and the planetary gear set.

Simulation model of planetary gearbox

A planetary gearbox simulation model was developed using commercial software (RomaxDesigner, 2017). To define the stiffness of the gears, the macro-geometry, such as the number of the teeth, the module, and the pressure angle, and the micro-geometry, such as the crowning and the lead slope, were considered. To define the non-linear stiffness of the bearing, the internal shape dimensions, such as the number and diameter of the balls or the rollers, and the diameter and curvature of the inner and the outer raceway of the bearing, were considered.

In addition, not only the geometric elements of the bearing but also the contact between the inner and outer raceways and the ball or roller, which is the non-linear effect of the internal clearance, and the pre-load were considered as factors related to the non-linear stiffness of the bearing (Park et al., 2015; Park et al., 2013).

Figure 4 and Figure 5 present the simulation model of the electric forklift gearbox. Figure 4 shows the model including the housing, and Figure 5 shows the model without the housing. The stiffness of complex shapes such as the web of a driven gear of the parallel shaft gear set, the carrier of the planetary gear set, and the housing

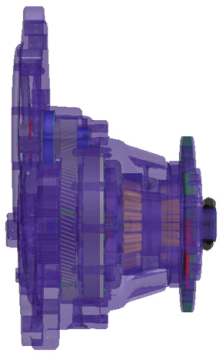

Figure 4. Entire model of the gearbox with FE housing.

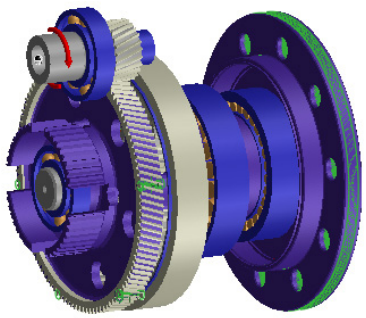

Figure 5. Entire model of the gearbox without FE housing.

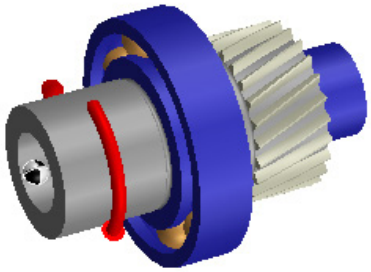

Figure 6. Drive gear, shaft, and bearings in the simulation model.

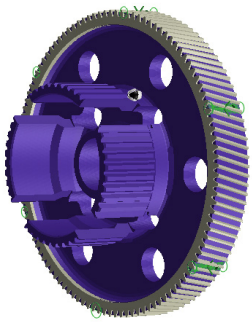

Figure 7. Driven gear and FEM web in the simulation model.

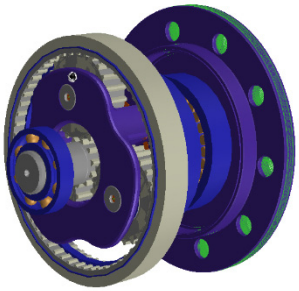

Figure 8. Planetary gear set, FEM carrier, wheel adapter, and bearings in the simulation model.

was input with finite element models. The torque and speed input to the drive gear of the parallel shaft gear set is 204 Nm @ 1000 RPM that is the rated torque and speed of the input shaft. The direction of rotation is clockwise with respect to the input shaft. The load applied to the gearbox wheel mount, due to the reaction force of the weight of the wheel, is 74.4 kN. Figure 6 shows the models of the drive gear, shaft, and bearings of the parallel shaft gear set. The red arrow indicates the torque. In Figure 7, the driven gear and FE (Finite Element) web of the parallel shaft gear set in the simulation model is illustrated. The planetary gear set, the FE carrier, the wheel mount, and the bearings of the simulation model are shown in Figure 8.

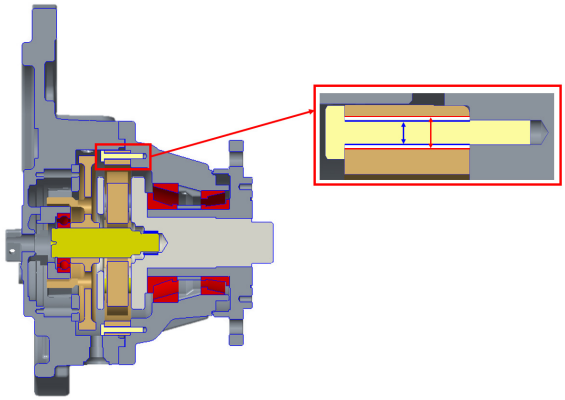

Figure 9. Radial clearance between ring gear and housing.

Analysis condition of simulation

Uneven load sharing affects the dynamic behavior and durability of a planetary gear set. The dynamic behavior is caused by vibration generated by irregular forces. The durability is affected because a larger load than the design load acts on the gear. One solution to this problem is to use an elastic support designed to offset fabrication and assembly errors in planet gears, or an elastic ring gear designed to withstand deformation-causing uneven loads (Iglesias et al., 2017). In this study, however, we investigated the degree of improvement in load sharing of a planetary gear set with the application of a floating ring gear.

The simulation model was divided into a model in which the ring gear was fixed to the housing (hereinafter referred to as the fixed ring gear model) and a model in which the radial clearance was applied between the ring gear and the housing (hereinafter referred to as the floating ring gear model). Figure 9 shows the radial clearance between the ring gear and the housing that is the difference between the diameter of the bolt hole on the ring gear (red arrow) and the diameter of the thread (blue arrow). In the fixed ring gear model, the radial clearance between the ring gear and the housing was set to 0 μm. In the floating ring gear model, the radial gap between the ring gear and the housing was increased from 10 μm to 100 μm in 10 μm increments.

Load sharing factor of planetary gear set

The load sharing of a planetary gear set is represented by load sharing factor, K_γ , as shown in equation (1) (ANSI/AGMA 6123-B06). Because the planet gears are assumed to rotate at the same speed, the load sharing factor could be calculated by multiplying the numerator and deno-

minator of equation (1) by the angular speed. Therefore, the load sharing factor could be defined as shown in equation (2).

Theoretically, a planetary gear set has uniform load sharing, and the load sharing factor is 1.0. However, due to various causes such as deformation and misalignment of gear, shaft, and bearing, as well as manufacturing error, the actual load on the planetary gear set is not uniformly divided in the planetary gear set, and the load sharing factor becomes greater than 1.0.

$$K_\gamma = \frac{T_{Branch} N_{CP}}{T_{Nom}} \quad (1)$$

$$K_\gamma = \frac{P_{max}}{P_{avg}} \quad (2)$$

Results and Discussion

We conducted the simulation for the fixed ring gear model and the floating ring gear model of an electric forklift gearbox at the operating speed and torque. The static deformation of the shafts, gears, and bearings was calculated considering the elasticity of the web of the driven gear of the parallel shaft gear set, carrier, and housing. Based on these parameters, the load sharing factor of the planetary gear set was calculated. However, in this study, the simulation was performed under the condition that there were no manufacturing or assembly errors in the planetary gear set.

The load sharing of the planetary gear set was evaluated by load sharing factor, K_γ . In this study, the load sharing factor was calculated by equation (2) after the power input to each planet gear was analyzed using commercial software (RomaxDesigner, 2017). For each model, the analytical condition was assumed a quasi-static process. Therefore, the carrier rotated from 0° to 360° at 60° increments, and the power flow was analyzed according to the position of each planet gear. Figure 10 presents the position of the planet gears in the planetary gear set when the carrier rotated 0°. The direction of rotation of the carrier was clockwise.

Fixed ring gear model

Figure 11 shows the result of the power flow analysis based on the position of each planet gear through one revolution in the fixed ring gear model. Because the analysis was conducted using the quasi-static assumption, the power varied according to the position of the planet gear, but the same power was input to the planet gears at the same position.

In the fixed ring gear model, when the carrier rotated 0° and 240°, the load sharing factor was the smallest. When the carrier rotated 0°, the power of planet gear 1 was 3.752 kW, the power of planet gear 2 was 3.279 kW, and the power of planet gear 3 was 3.805 kW. The maximum power was 3.805 kW for planet gear 3, and the average power was 3.612 kW, so that K_γ was calculated to be 1.053. When the carrier rotated 240°, the power of planet gear 1 was 3.805 kW, the power of planet gear 2 was 3.752 kW, and the power of planet gear 3 was 3.279 kW. The maximum power was 3.805 kW for planet gear 1, and the average power was 3.612 kW, so that K_γ was calculated to be 1.053.

In the fixed ring gear model, when the carrier rotated 60°, the load sharing factor was the largest. In this case, the power of planet gear 1 was 3.377 kW, the power of planet gear 2 was 3.492 kW, and the power of planet gear 3 was 3.967 kW. The maximum power was 3.967 kW for planet gear 3, and the average power of the planet gear was 3.612 kW, so that K_γ was calculated to be 1.098. K_γ

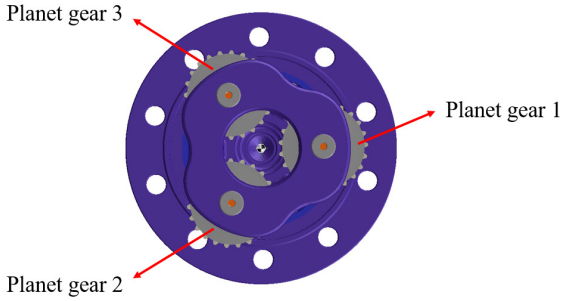

Figure 10. Position of planet gears in planetary gear set when the carrir rotated 0°

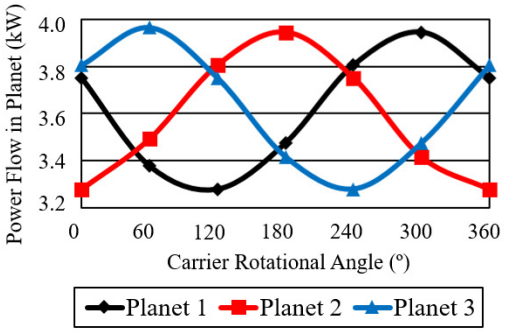

Figure 11. Power flow in planets of fixed ring gear model.

increased by about 4% compared to the minimum value.

The smallest power input to the planet gear per revolution was 3.279 kW, and the largest power was 3.967 kW, which represents an increase of about 21%. Because each planet gear rotated at the same angular speed, the power input to each planet gear was proportional to the torque. Therefore, the fact that the power fluctuation was large indicated that the variation in the load generated in the planet gear was also large. The reason for this phenomenon was that the position of planet gear 1, 2, and 3 changed when the carrier rotated in the quasi-static state, while the vertical load applied to the tire from the ground did not changed.

Floating ring gear model

Figures 12-21 show the results of the power flow analysis based on the position of each planet gear through one revolution in the floating ring gear model. Similar to the analysis results of the fixed ring gear model, the power of each planet gear changed according to the position, under the analysis conditions, but the power was the same for every cycle of the carrier.

Figure 12 shows the result when the 10 μm clearance was applied to the floating ring gear model. When the carrier rotated 0°, K_γ reached its minimum value of 1.047, and when the carrier rotated 180°, K_γ reached its maximum value of 1.081, an increase of about 3%. The maximum power input to the planet gear was 3.903 kW, and the minimum power was 3.322 kW. Therefore, the maximum load on the planet gear was about 17% larger than the minimum load.

Figure 13 shows the result when the 20 μm clearance was applied to the floating ring gear model. When the carrier rotated 0°, K_γ reached its minimum value of 1.040, and when the carrier rotated 180°, K_γ reached its maximum value as 1.067, an increase of about 2.6%. The maximum power input to the planet gear was 3.852 kW, and the minimum power was 3.372 kW. Therefore, the maximum load generated on the planet gear was about 14% larger than the minimum load.

Figure 14 shows the result when the 30 μm clearance was applied to the floating ring gear model. When the carrier rotated 0°, K_γ reached its minimum value of 1.032, and when the carrier rotated 180°, K_γ reached its maximum value of 1.052, an increase of about 2%. The maximum power input to the planet gear was 3.800 kW, and the minimum power was 3.425 kW. Therefore, the maximum load generated on the planet gear was about 14% larger than the minimum load.

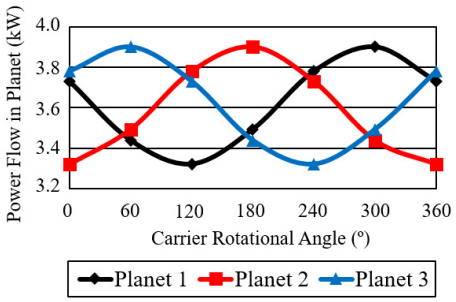

Figure 12. Power flow in planet gears of floating ring gear model with 10 μm

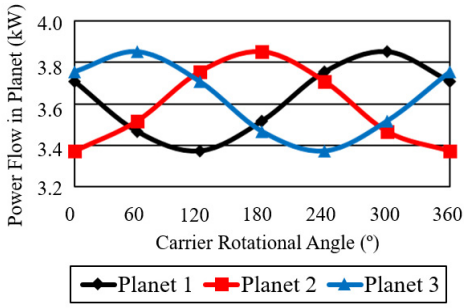

Figure 13. Power flow in planet gears of floating ring gear model with 20 μm clearance.

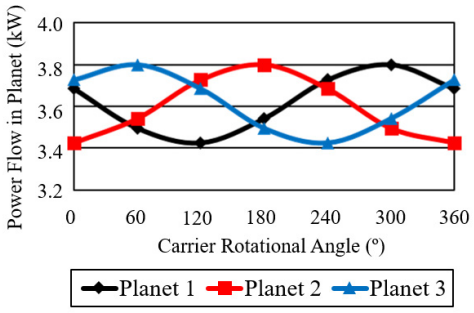

Figure 14. Power flow in planet gears of floating ring gear model with 30 μm

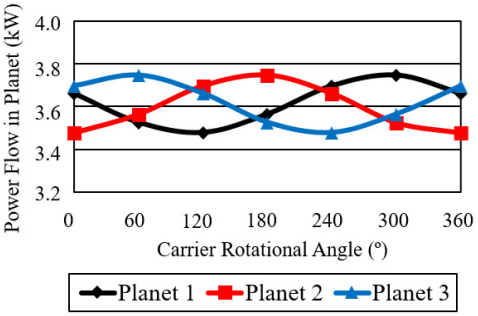

Figure 15. Power flow in planet gears of floating ring gear model with 40 μm

Figure 15 shows the result when the 40 μm clearance

was applied to the floating ring gear model. When the carrier rotated 0°, K_γ reached its minimum value of 1.023, and when the carrier rotated 180°, K_γ reached its maximum value of 1.037, which was an increase of about 1.4%. The maximum power input to the planet gear was 3.747 kW, and the minimum power was 3.478 kW. Therefore, the maximum load generated on the planet gear was about 8% larger than the minimum load.

Figure 16 shows the result when the 50 μm clearance was applied to the floating ring gear model. When the carrier rotated 0°, K_γ reached its minimum value of 1.015, and when the carrier rotated 180°, K_γ reached its maximum value of 1.022, which was an increase of about 0.7%. The maximum power input to the planet gear was 3.693 kW, and the minimum power was 3.532 kW. Therefore, the maximum load generated on the planet gear was about 4.6% larger than the minimum load.

Figure 17 shows the result when the 60 μm clearance was applied to the floating ring gear model. When the carrier rotated 0°, K_γ reached its minimum value of 1.006, and when the carrier rotated 180°, K_γ reached its maximum value of 1.008, which was an increase of about 0.2%. The maximum power input to the planet gear was 3.641 kW, and the minimum power was 3.585 kW.

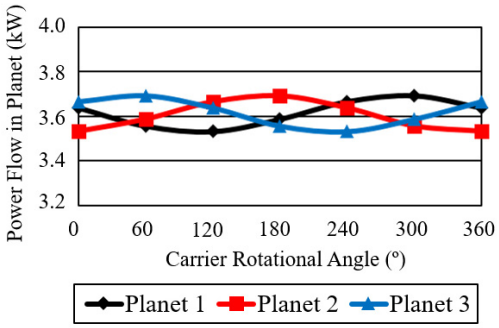

Figure 16. Power flow in planet gears of floating ring gear model with 50 μm clearance.

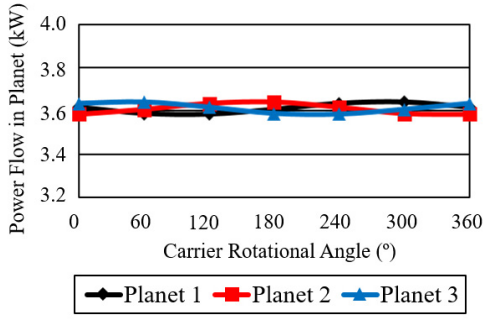

Figure 17. Power flow in planet gears of floating ring gear model with 60 μm clearance.

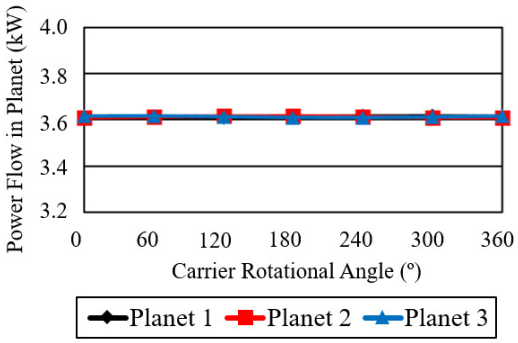

Figure 18. Power flow in planet gears of floating ring gear model with 70 μm clearance.

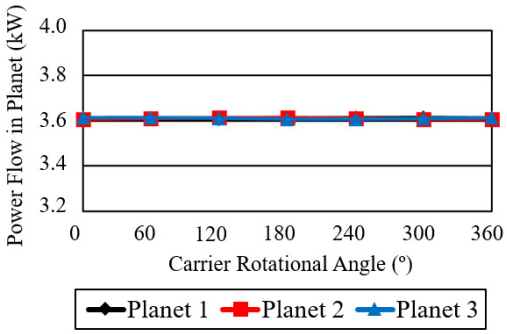

Figure 19. Power flow in planet gears of floating ring gear model with 80 μm clearance.

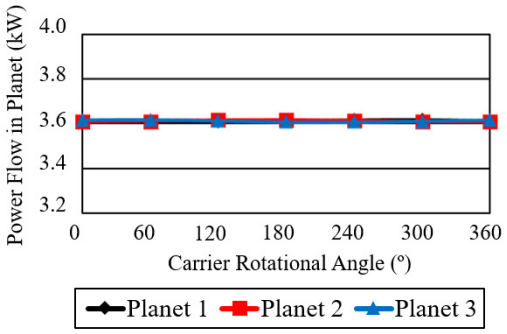

Figure 20. Power flow in planet gears of floating ring gear model with 90 μm clearance.

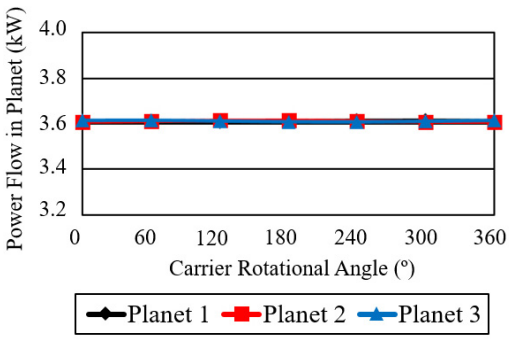

Figure 21. Power flow in planet gears of floating ring gear model with 100 μm clearance.

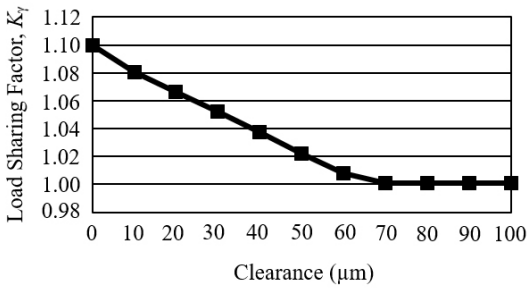

Figure 22. Maximum load sharing factor of the models according to the clearance size.

Therefore, the maximum load generated on the planet gear was about 1.6% larger than the minimum load.

Figures 18-21 shows the analytical results when clearances of 70 μm, 80 μm, 90 μm, and 100 μm were applied to the floating ring gear model, respectively. Under the four analytical conditions, K_γ was constant at 1.001, regardless of the carrier angle of rotation. The maximum power input to the planet gear was 3.616 kW, and the minimum power was 3.608 kW.

Based on these results, the maximum value of the load sharing factor of the model according to the size of the clearance was plotted on the graph as shown in Figure 22. It was confirmed that the planetary gearbox used in this study could have the fully floating ring gear when the radial clearance between the housing and the ring gear was 70 μm. The use of the fully floating ring gear resulted in uniform load sharing of the planetary gear set and a significant reduction in the load variation of the planet gear. This was also consistent with the findings of Singh (2010), who found that increasing the clearance above 70 μm did not affect the load sharing of planetary gear sets.

Conclusions

In this study, the fixed ring gear model and floating ring gear model were constructed with reference to the planetary gearbox used in actual industry. The influence of the floating ring gear on the load sharing of the planetary gear set was analyzed through the simulation. The load sharing of the planetary gear set was evaluated by load sharing factor, K_γ .

From the simulation results of the load sharing of the fixed ring gear model and the floating ring gear model, K_γ was calculated to be 1.001 for a radial clearance between the housing and the ring gear of 70 μm. In other words, the load was divided almost evenly in the planetary gear set. This means that for the planetary gearbox model used in this study, a 70 μm clearance between the housing and the ring gear was required to realize a fully floating ring gear. In addition, when a clearance of 70 μm or greater was applied, it was confirmed that the size of the clearance did not affect the K_γ of the planetary gear set.

This study showed that the use of a fully floating ring gear increased the power density by uniformly dividing the load of the planetary gear set. Thus, the fully floating ring gear was expected to reduce the size of the gearbox. In the agricultural machinery, a planetary gear set is used in the hydro-mechanical transmission (HMT) and the final drive. In addition, if agricultural machinery becomes electrified, a planetary gear set could be applied to develop its automatic transmission. Therefore, a fully floating ring gear could be used to the agricultural machinery now and also in the future.

However, in this study, because the simulation was conducted under the condition that there were no manufacturing or assembly errors in the planetary gear set, there was the limitation that the load sharing factor did not deviate greatly from unity, even in the fixed ring gear model. In future research, an analysis including manufacturing and assembly errors will be performed and then compared to the results of this study. The simulation model will be also validated using a gearbox produced in the same manner as the simulation model.

Conflict of Interest

The authors have no conflicting financial or other interests.

Acknowledgement

This research was financially supported by the Ministry of Trade, Industry, and Energy (MOTIE), Korea, under the "Regional industry based organized support program" (reference number R0006268) supervised by the Korea Institute for Advancement of Technology (KIAT). This study was conducted by using RomaxDESIGNER of Romax Technology Ltd.

References

ANSI/AGMA. 2006. ANSI/AGMA 6123-B06: Design Manual for Enclosed Epicyclic Gear Drives. Virginia, USA: American National Standards Institute/American Gear Manufacturers Association.

Bayindir, K. Ç., M. A. Gözüküçük and A. Teke. 2011. A comprehensive overview of hybrid electric vehicle: Powertrain configurations, powertrain control techniques and electronic control units. Energy Conversion and Management 52(2): 1305-1313. https://doi.org/10.1016/j.enconman.2010.09.028

Bodas, A. and A. Kahraman. 2004. Influence of carrier and gear manufacturing errors on the static load sharing behavior of planetary gear sets. JSME International Journal Series C Mechanical Systems, Machine Elements and Manufacturing 47(3): 908-915. https://doi.org/10.1299/jsmec.47.908

Iglesias, M., A. Femandez del Rincon, A. de-Juan, P. Garcia, A. Diez-Ibarbia and F. Viadero. 2017. Planetary transmission load sharing: Manufacturing errors and system configuration study. Mechanism and Machine Theory 111: 21-38. https://doi.org/10.1016/j.mechmachtheory.2016.12.010

Kahraman, A. 1994. Load sharing characteristics of planetary transmissions. Mechanism and Machine Theory 29(8): 1151-1165. https://doi.org/10.1016/0094-114X(94)90006-X

Kahraman, A. and S. Vijayakar. 2001. Effect of internal gear flexibility on the quasi-static behavior of a planetary gear set. Journal of Mechanical Design 123(3): 408-415. https://doi.org/10.1115/1.1371477

Kim, J. G., Y. -J. Park, G. H. Lee, J. Y. Oh and Y. J. Kim. 2017. A study on the load sharing among planet gears according to the phase of carrier pinhole position error in the planetary gearbox. Journal of the Korean Society of Precision Engineering 34(6): 377-382 (In Korean, with English abstract). https://doi.org/10.7736/KSPE.2017.34.6.377

Kim, J. -H. and D. -I. D. Cho. 1997. An automatic transmission model for vehicle control. In: *Proceedings of Conference on Intelligent Transportation Systems*, pp. 759-764. Boston, MA, USA: November 1997.

Kim, T. -H., S. -J. Lee and W. Choi. 2011. Design and control of the phase shift full bridge converter for the on-board battery charger of the electric forklift. In: *8th International Conference on Power Electronics - ECCE Asia*, pp. 2709-2716. Jeju, South Korea: May -June 2011.

Nejad, A. R., Y. Xing, Y. Guo, J. Keller, Z. Gao and T. Moan. 2015. Effects of floating sun gear in a wind turbine's planetary gearbox with geometrical imperfections. Wind Energy 18(12): 2105-2120. https://doi.org/10.1002/we.1808

Noh, S. Y., L. S. Kim., S. H. Cho and S. K. Lyu. 2017. Study on the tooth micro-geometry optimization of planetary gear for drive reducer. Journal of the Korean Society for Precision Engineering 34(6): 371-376 (In Korean, with English abstract). https://doi.org/10.7736/KSPE.2017.34.6.371

Park, S. M., T. W. Park, S. H. Lee, S. W. Han and S. K. Kwon. 2010. Analysis study to estimate the performance of the power shift drive (PSD) axle for a forklift. International Journal of Automotive Technology 11(1): 49-56. https://doi.org/10.1007/s12239-010-0007-3

Park, Y.-J., J.-G. Kim, G.-H. Lee and S. B. Shim. 2015. Load sharing and distributed on the gear flank of wind turbine planetary gearbox. Journal of Mechanical Science and Technology 29(1): 309-316. https://doi.org/10.1007/s12206-014-1237-5

Park, Y.-J., G.-H. Lee, Y.-Y. Nam and J.-K. Kim. 2012. Influence of flexible pin for planets on service life of wind turbine gearboxes. Transactions of the Korean Society of Mechanical Engineers A 36(9): 953-960 (In Korean, with English abstract). http://dx.doi.org/10.3795/KSME-A.2012.36.9.953

Park, Y.-J., G.-H. Lee, J.-S. Song and Y.-Y. Nam. 2013. Characteristic analysis of wind turbine gearbox considering non-torque loading. Journal of Mechanical Design 135(4): 044501. https://doi.org/10.1115/1.4023590

RomaxDesigner. 2017. RomaxDesigner Software Manual. R17. Nottingham, UK: Romax Technology Ltd.

Shin, Y. I., C. H. Yoon, S. G. Han, S. G. Park and C. K. Song. 2016. Design improvement for a planetary gear system in hydraulic drive system. Journal of the Korean Society for Precision Engineering 33(10): 851-856 (In Korean, with English abstract). http://dx.doi.org/10.7736/KSPE.2016.33.10.851

Singh, A. 2010. Load sharing behavior in epicyclic gears: Physical explanation and generalized formulation. Mechanism and Machine Theory 45(3): 511-530. https://doi.org/10.1016/j.mechmachtheory.2009.10.009

Nomenclature

K_γ : Mesh load factor
T_{Branch}: Torque in branch with heaviest load (N-m)
T_{Nom}: Total nominal torque (N-m)
N_{CP}: Number of planets
P_{max}: Maximum value of power input to each planet
P_{avg}: Average power of planets